J Mater Sci (2008) 43:5474–5482
DOI 10.1007/s10853-008-2840-6

Comparative study of heat-affected zone with weld and base material after post-weld heat treatment of HSLA steel using ball indentation technique

Sabita Ghosh · T. K. Pal · Surojit Mukherjee · Goutam Das · Sukomal Ghosh

Received: 14 May 2007 / Accepted: 25 June 2008 / Published online: 16 July 2008

Abstract Ball indentation technique (BIT) is employed to study the effect of post-weld heat treatment on the mechanical properties of a high strength low alloy (HSLA) steel and subsequently on the quality of the weldment. Well-defined load-deflection curves and corresponding true stress–strain curves for different zones (base, HAZ, weld) of sectioned sample (top and middle) and their validation with mechanical properties obtained by conventional method established the effectiveness of the present ball indentation (BI) set up. Investigations on microstructure of all the zones have been carried out to find out a correlation with the obtained mechanical properties. Evaluation of the mechanical properties of materials through BIT could characterize the heat-affected zone in weld HSLA steel.

Introduction

The weld joints embedded in the structures or components are expected to accomplish certain service-related capabilities or properties. In weld materials, weld zone and heat-affected zone (HAZ) are themselves composed of a multitude of metallurgical structures as well as chemical heterogeneity often differing from the base metal [1]. In a weld joint, the response of the area next to the fusion line is quite dependent on the nature of the material as well as on the welding parameters or procedure adopted. A variation in properties is thus expected throughout the weld joint. The properties of weld metal and base metal may be evaluated through conventional mechanical test by slicing a specimen from the region of interest. However, the HAZ is usually too small to carry out conventional test. Characterization of HAZ is equally important as that of weld area because a significant difference in strength may cause crack initiation in the component. Usually, the post-weld heat treatment is a measure to avoid such a crack initiation and subsequent failure.

The appearance of fine cracks in the weld area is also ascribed to the presence of hydrogen in weld metal. The 'atmosphere' is considered to be the chief source of hydrogen introduction besides the possible sources of contamination by grease, oil at the joining surface, or use of unbaked electrode during welding. With the dissociation of moisture at the arc temperature, the hydrogen is carried on by the arc column and is entrapped in the weld metal and accumulates in micro voids. On exceeding the yield strength of materials, the pressure inside the voids causes voids to burst and results in the formation of micro cracks. Subsequent coalescence of these cracks and their propagation may even lead to material failure [1].

While addressing the stress cracking behavior, it was reported [2, 3] that, in electron beam welded high grade super-martensitic stainless steel (SMSS) with matching consumables, the microstructure/composition of the weld metal exhibited a significant influence of the hydrogen pick-up that resulted in the hydrogen-induced brittle failure in the weld region. Further, the hydrogen-induced embrittlement may occur due to redistribution of the lattice hydrogen atoms by the strain-induced dislocations, as reported by Brass et al. [4]. In addition, interfaces such as grain boundaries and second phases behave like dislocation arrays and thus accumulate solute hydrogen. It reduces the

S. Ghosh (✉) · G. Das · S. Ghosh
National Metallurgical Laboratory, Jamshedpur 831 007, India
e-mail: sabita_ghosh@rediffmail.com

T. K. Pal · S. Mukherjee
Jadavpur University, Kolkata, India

mobility of the dislocations and results in the embrittlement of the interface. Also, it may form hydride/new phases either with the solvent atoms or some other solute element [5].

The ball indentation technique (BIT) has several features and it has certain advantages over the conventional mechanical test [6]. One of the main features is that the test technique is localized. The spatial variations in properties can be determined by this technique and thus finds application in evaluation of mechanical properties of weld and HAZ. By using BIT, Murty et al. [7] evaluated local tensile and fracture properties of the weld SA-533B steel, across the regions, such as the base metal, HAZ, and the weld metal having different microstructure. It was observed that the gradients in the yield and tensile strengths of different zones were consistent with the changes in the microstructures. The results obtained through BIT for base and weld metals compared favorably with the results from conventional mechanical test [7]. Using in situ approach of stress–strain microprobes (SSM) to evaluate damage in ageing aircraft [8], the results of the automated ball indentation (ABI) showed that the flow properties measured by the microprobes at three circumferential weld areas were in good agreement and were consistently lower than those at the base metal and HAZ test locations. The ABI test technique was applied to measure the 'through-the-thickness' variations of mechanical properties in the pressure vessels, wherein the location dependence of mechanical property was established [9].

During an indentation test, on application of load, the material around the area of contact between the indenter (ball) and the specimen may either pile-up or sink-in. Since original development of the Oliver–Pharr model [10], the estimation of the contact area has undergone many alterations and refinements to improve its accuracy on consideration of the pile-up phenomenon [11, 12].

The contemplation of pile-up/sink-in in materials has significant influence on the measurement of indentation diameters (both total and plastic); if set aside, the result may deviate from actual. Field and Swain [13] have used sub-micrometer-sized spherical micro-indenter to determine the stress–strain behavior of a bulk material. Stepwise indentation with partial unloading was used to separate the elastic and plastic components of indentation. They considered the "piling up" or "sinking in" phenomenon to determine the actual contact depth. The extension and the height of the accumulation of the substance were found to be independent of the size of the impression [14], yet, depending on the work-hardening characteristics of the materials. Bolshakov and Pharr [11] have reported the investigation on the influence of pile-up on accurate measurement of hardness and elastic modulus by finite element simulation of a conical indenter. They postulate that when pile-up is large, the areas deduced from analyses of load–displacement curves underestimate the true contact areas by as much as 60%. That a correction factor is necessary to introduce to the load-depth measured plastic depth to assess the actual contact area between the indenter and the test material has been the finding of various researchers [13, 15–18].

The present work aims to characterize HSLA steel in weld as well as post-weld heat-treated condition using an in-house developed BI test set up. The work has also been directed to demonstrate the capability of the present BI system for assessment of the localized mechanical properties of the HSLA steel across various weld regions such as base metal, HAZ, and the weld zone having definite microstructure. Attempt is also made to determine the variation in mechanical properties at the top and middle of the weld, HAZ and base material and validate them through test results obtained from conventional test.

Theoretical approach

The BIT uses multiple indentations by a spherical indenter on a metal surface at a single test location. The spherical ball is indented with a pre-determined rate of loading and multiple indentations are made at a fixed location using several steps of loading–unloading–reloading sequence. The load increases approximately linearly with the penetration depth. On application of load, two non-linear processes occur simultaneously, which oppose the action of each other. One of these is the non-linear increase in the applied load with indentation depth due to non-linear geometry of the spherical indenter and another is the non-linear increase of load with indentation depth due to work hardening of the test pieces. During each subsequent loading, more segment of material beneath the indenter endures plastic deformation, thus continuous yielding and strain hardening occur simultaneously. In contrast, for the case of a uni-axial tensile test, the plastic deformation is confined only to the limited volume of test sample of gauge section. For each loading cycle the total depth (h_t) is measured while the load is applied and the plastic depth (h_p) is measured after completing unloading. The computer program determines the slope of each unloading cycle. Then the intersection of this line with the zero load line determines the value of h_p. The h_t, h_p, and the corresponding loads in N are the raw data for determining the mechanical properties like ultimate tensile strength (UTS), yield strength (YS), strength coefficient (K), strain hardening exponent (n), and true stress–true strain (σ_t–ε_t) curve. The details of the theory and advantages of the technique are given elsewhere [7, 16, 19–24].

Experimental procedure

The material used in the present investigation was ASME A517 Gr.F HSLA steel. The electrode used for the welding process was AWSE 11018M, Basicoat. The schematic of the weld sample is shown in Fig. 1. The dimension of the weld portion was 30 mm in width, 2 mm root gap, i.e. 30 mm for the top sample and 2–3 mm for the root sample. The original size of the weld plate was 600 × 320 × 38 mm^3. The nominal composition of base metal, weld metal at the top and middle positions is given in Table 1. Three weld specimens were chosen for the investigation. These were designated as '1', '2', and '3'. Specimen '2' and '3' were given post-weld heat treatment, '2' at 650 °C for 95 min and '3' at 250 °C for 120 min. The test samples were sectioned from top and middle portion of each specimen.

Samples were separately sectioned from top and middle position (Fig. 1) of the weld material for both BI and conventional tensile test. Conventional tests were performed on the base and weld samples only. For conventional test, the specimens were made as per ASTM standard (ASTM 8M). The conventional tests were carried out using an INSTRON mechanical testing machine. For BI test, samples of size 30 × 15 × 10 mm^3 were cut from base and weld zone and also from the part where the entire weld, HAZ, and base zone existed.

The detail of the BI set-up and experimental procedure is given elsewhere [25]. Due to the formation of pile-up in materials at the surrounding of contact surface, the LVDT measured contact area differs from the actual contact area of the indentation. In earlier investigations by the authors [18, 25–28], the pile-up phenomenon had due consideration in evaluation of mechanical properties. It was observed that the extent of accumulation of the piled up material was influenced by the work hardening characteristic of the materials. They also [27] incorporated a correction factor on the basis of morphology of pile-up/sink-in and yield ratio parameter of the materials in relation to indentation diameter. In the present investigation also, the pile-up/sink-in phenomenon has been considered. In a few cases the plastic diameters (d_p) are measured directly using optical microscope. To accomplish this, indentations are made at several locations on the test surface at a load close to the LVDT displayed load. A FORTRAN-based program has been developed for the analysis of BI test results.

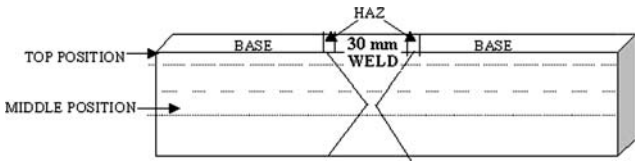

Fig. 1 Schematic of the investigated welded sample

Table 2 Comparison of UTS, YS, K, and n values obtained from conventional and BI test

Conventional test results (BI test results)				
Sample ASME A517	UTS (MPa)	YS (MPa)	K (MPa)	n
1 Base	817	763	–	–
	(819)	(737)	(1103)	(0.085)
'1' Middle HAZ	(768)	(721)	(1066)	(0.099)
'1' Middle weld	775	648	1146	0.097
	(816)	(578)	(1129)	(0.098)
'1' Top HAZ	(804)	(722)	(1185)	(0.075)
'1' Top weld	807	685	1163	0.086
	(809)	(608)	(1185)	(0.096)
'2' Base	816	773	1000	0.058
	(808)	(762)	(1018)	(0.06)
'2' Middle HAZ	(727)	(750)	(970)	(0.063)
'2' Middle weld	669	565	999	0.098
	(672)	(502)	(926)	(0.095)
'2' Top HAZ	(760)	(725)	(930)	(0.05)
'2' Top weld	840	717	1108	0.089
	(834)	(679)	(1103)	(0.08)
'3' Base	819	781	–	–
	(827)	(761)	(1074)	(0.07)
'3' Middle HAZ	(811)	(743)	(1089)	(0.086)
'3' Middle weld	781	650	1176	0.086
	(834)	(597)	(1144)	(0.095)
'3' Top HAZ	(749)	(709)	(996)	(0.08)
'3' Top weld	857	725	1207	0.085
	(900)	(714)	(1214)	(0.087)

Table 1 The elemental composition of the base metal, weld metal at the top and middle position (in wt.%)

	C	Mn	Si	S	P	Ni	Cr	Mo	V	B	Cu	Fe
Base	0.015	0.825	0.25	0.035	0.035	0.85	0.525	0.50	0.55	0.0005	0.325	Bal.
Weld top	0.088	1.535	0.403	0.038	0.385	1.975	0.036	0.346	0.002	Trace	0.012	Bal.
Weld middle	0.136	1.865	0.481	0.244	0.2445	0.2645	2.359	0.252	0.567	Trace	0.084	Bal.

Table 3 Comparison of UTS (in MPa) for base, weld, and HAZ obtained from conventional and BI test

Position of the sample	Sample '1'		Sample '2'		Sample '3'	
	Top	Middle	Top	Middle	Top	Middle
Base (conventional)	817	–	816	–	819	–
(BIT)	819	–	808	–	827	–
Weld (conventional)	807	775	840	669	857	781
(BIT)	809	816	834	672	900	834
HAZ (BIT)	804	768	760	727	749	811

Results and discussion

The flow properties of the base and weld zone of all the investigated samples, determined through BIT and conventional technique, are shown in the Table 2. Since it is unfeasible to determine the mechanical properties of HAZs through conventional technique, only BIT obtained values are listed in this table. Also, extracts from this table are further compiled in Table 3 to portray the ultimate tensile strength in particular for the purpose of comparison.

Base and weld zone

Top and middle portion of all the samples were studied in consideration of their flow properties using BIT and conventional technique along with their microstructures. The P–δ curves for top section and their corresponding SEM micrographs for base, HAZ, and weld zone for all samples are shown in Figs. 2–4. The observed microstructures are almost similar (martensitic) except in HAZ of sample '3' (tempered martensitic). The overall variation in obtained values of σ_{uts} and σ_y from the BIT and conventional techniques is found to be small (Table 2). Incidentally, for all three samples, the observed deviation in the values of σ_{uts} obtained through BIT and conventional techniques is within 1% for base and that for weld zone is within 6%.

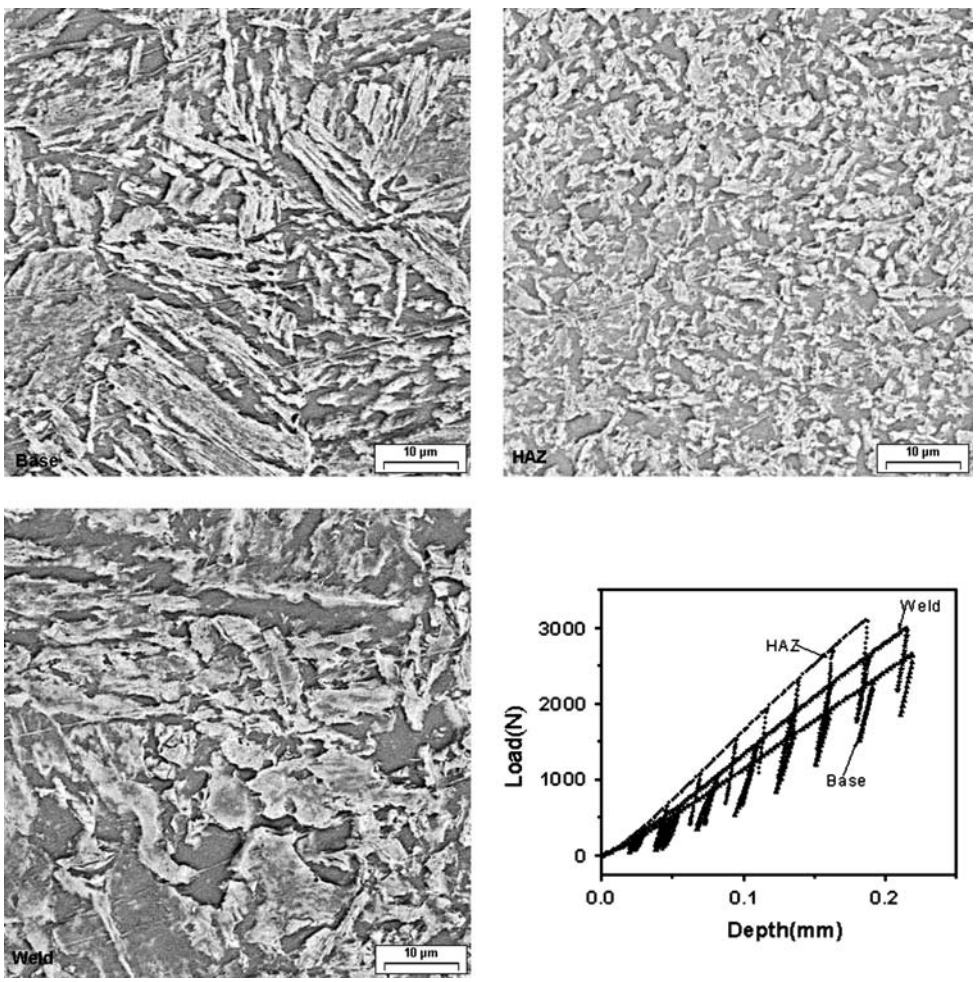

Fig. 2 Microstructure of base, HAZ, weld, and corresponding P–δ curves for the top surface of the sample '1'

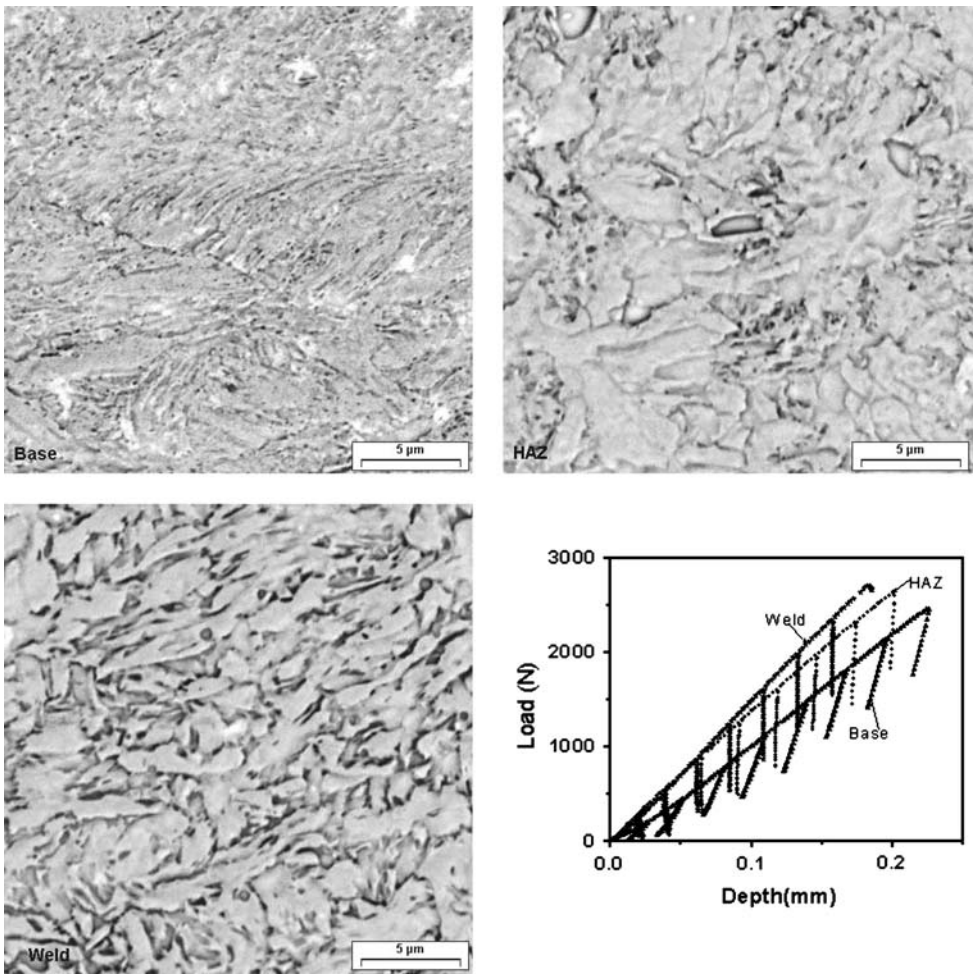

Fig. 3 Microstructure of base, HAZ, weld, and corresponding P–δ curves for the top surface of the sample '2'

The depicted P–δ curves in Figs. 2–4 explain the material characteristics. It is evident that a change in slope of the curve is an indication of material's resistance to indentation. To produce the same deformation, a higher load is required for a material that shows greater slope. Irrespective of samples, the base region exhibits the minimum slope. The highest slope is observed in sample '1' at HAZ region. Samples '2' and '3' show the weld region to exhibit the highest slope, the post-weld heat treatment of these samples, probably, reflect that HAZ to occupy the intermediate position. With different BI load–displacement traces, the yield strengths vary for base and weld region, while σ_{uts} do not change significantly except for the middle section of the sample '2' (Table 3).

The flow properties are verified with conventional test results for weld and base position. Figure 5 shows the comparison of the σ_t–ε_p curves derived from BI and conventional tensile test for all the three samples at weld zone (top and middle positions). These are observed to be in close proximity.

Heat-affected zone

The micrographs (top portion) of HAZ of all the three samples are shown in Figs. 2–4. It is observed that the structure of sample '1' is tempered martensite while samples '2' and '3' show coarsening of martensite as a result of imparting post-weld treatment. On comparison, the σ_{uts} of HAZ for sample '1' is observed to be higher than that of samples '2' and '3' for the top surface (Fig. 6), which is in agreement with the observed microstructure. In the middle surface, however, sample '3' shows a little higher flow stress compared to samples '1' and '2' (Fig. 7). Based on the σ_t–ε_p curve, the individual samples (Fig. 8) are also compared for σ_{uts} in two positions, i.e. at the top and middle portion. The σ_{uts} of the top surface of samples '1' and '2' was observed to be higher in comparison to their middle portion. In the process of welding, a material is heated. The top portion of the HAZ dissipates heat faster compared to the middle portion that results in the higher strength at the top portion. The post-weld treatment (650 °C for 95 min) produces coarse martensite structure throughout the sample, resulting in lower

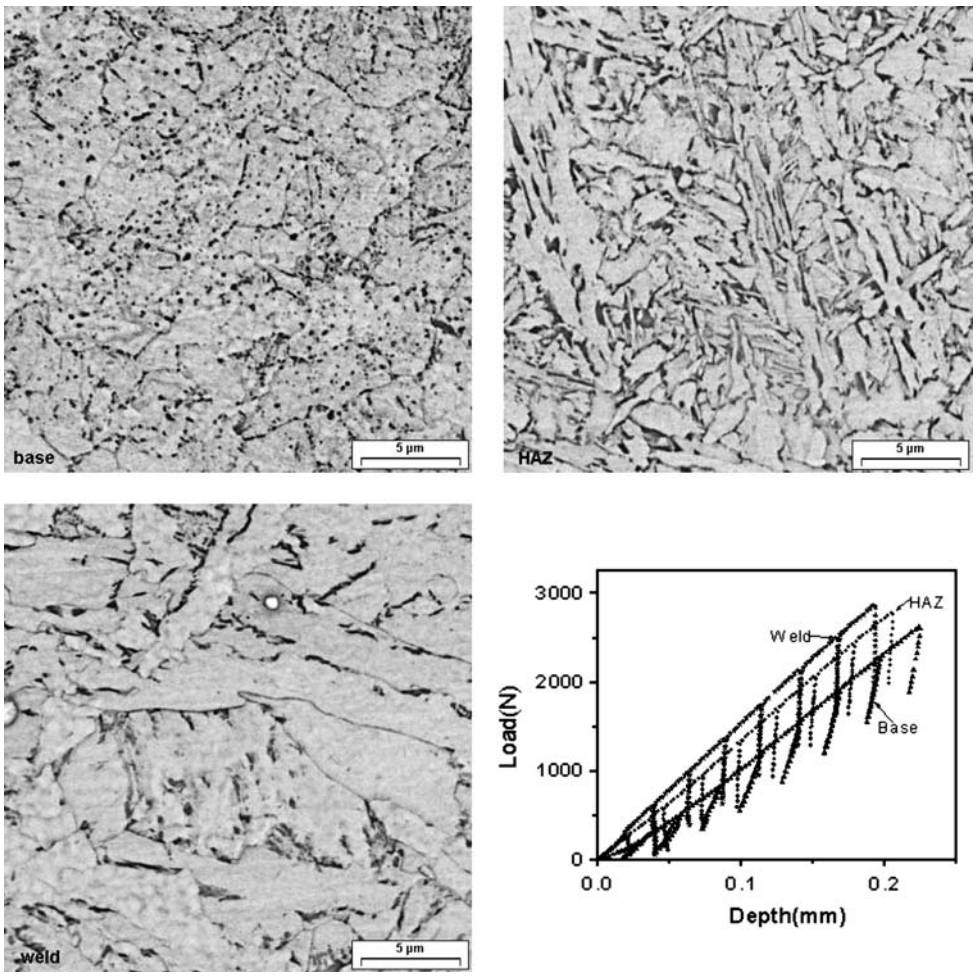

Fig. 4 Microstructure of base, HAZ, weld, and corresponding P–δ curves for the top surface of the sample '3'

σ_{uts} value compared to a tempered martensitic structure. The differential cooling rate appears to be responsible for a higher σ_{uts} in the top portion. By analogy, sample '3' should also have shown higher σ_{uts} in the top portion, yet it shows increased σ_{uts} in the middle portion in comparison to the top portion. This sample was post-weld treated at 250 °C for 120 min; the differences in microstructure (Fig. 9) between the two portions explain the result. The decreased σ_{uts} in the top portion is due to coarse tempered martensite structure (Fig. 9a) in contrast to the martensitic structure as observed in the middle portion (Fig. 9b). It appears that a post-weld treatment temperature of 250 °C for 120 min is inadequate to produce uniform microstructure in the two positions.

Overall it is observed that in HAZ, sample '1' shows higher flow properties in comparison to the other two heat-treated samples. It is found that though the values of σ_y are nearly the same for all materials in both positions (top and middle), but the σ_{uts}, 'K' and 'n' values are higher for sample '1' compared to samples '2' and '3'(Fig. 10).

The above findings advocate the capability of BIT of finding out the point-to-point variation of the mechanical properties of the weldment material as well as of characterizing HAZ.

Conclusion

Based on the results and discussion, the following inferences are drawn:

1. The results obtained through BIT and conventional technique are comparable (base and weld zone only).
2. The true stress–strain curves, determined from both BIT and conventional tests, are well matched.
3. All three samples show higher values of σ_{uts} in the weld region as compared to the HAZ. The disparity in strength (σ_{uts}) between the top weld and base metal was insignificant.
4. In the weld region, for all samples, the top portion shows higher strength (both σ_{uts} and σ_y) than the middle portion, which is in accordance with the observed microstructure.

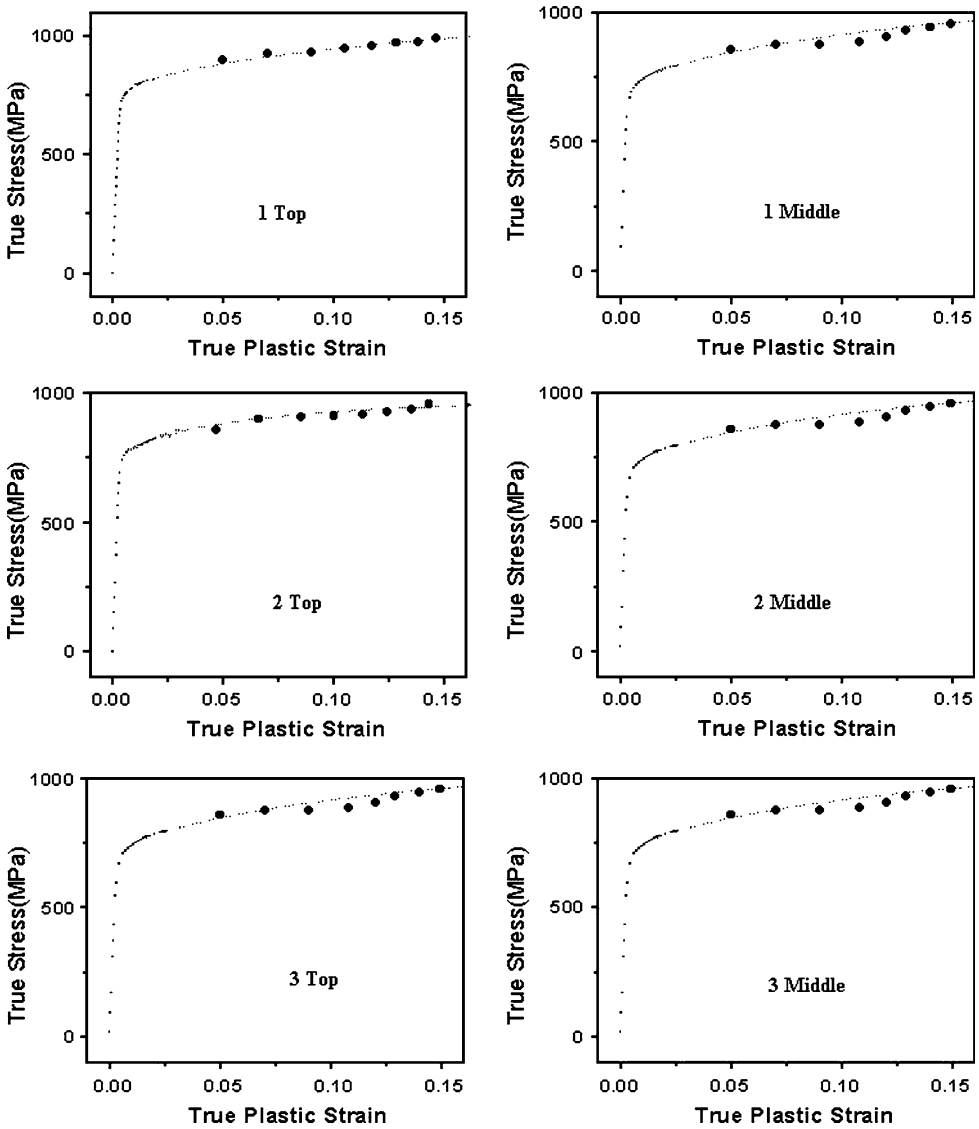

Fig. 5 The BIT obtained σ_t–ε_t curves and the conventional tensile test results for sample 1, 2, and 3 (top and middle) of weld zone (•••, BI test results; ···, conventional test results)

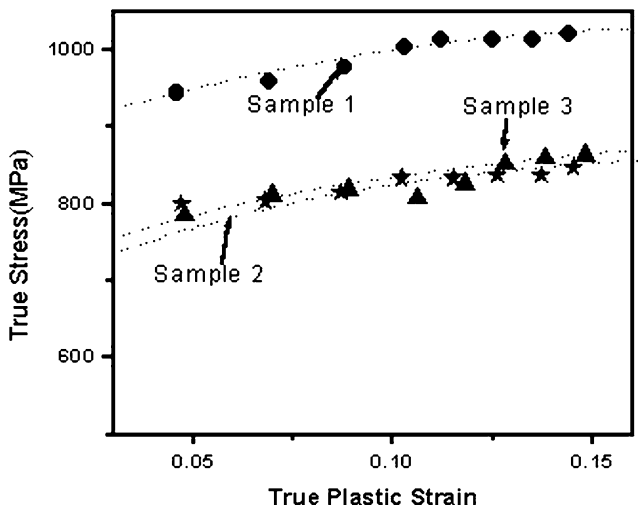

Fig. 6 σ_t–ε_t curves for the all three investigated samples for the top surface of the HAZ

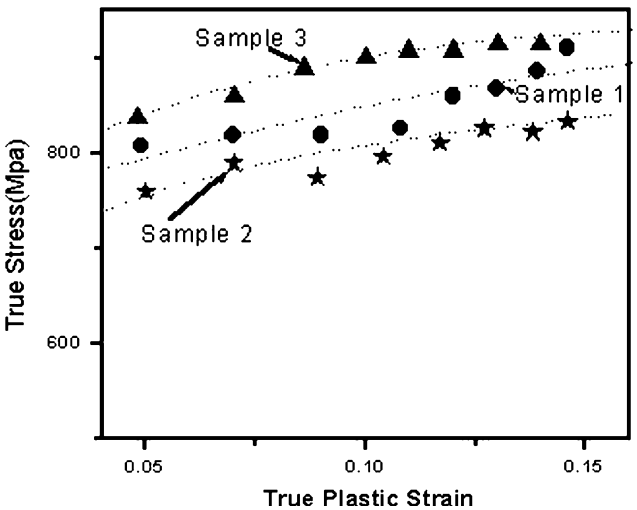

Fig. 7 σ_t–ε_t curves for the all three investigated samples for the middle position of the HAZ

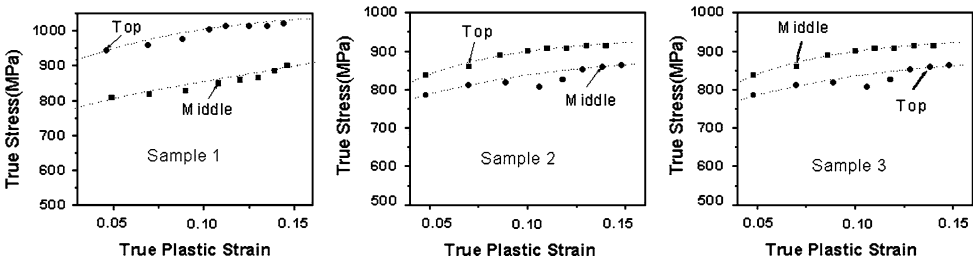

Fig. 8 True stress–strain curve for HAZ for samples '1', '2' and '3'

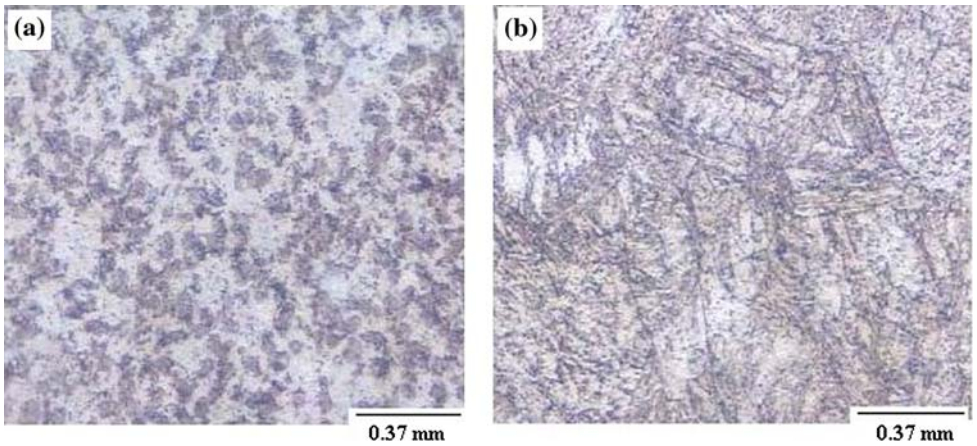

Fig. 9 Microstructures of sample '3': (**a**) top and (**b**) middle position

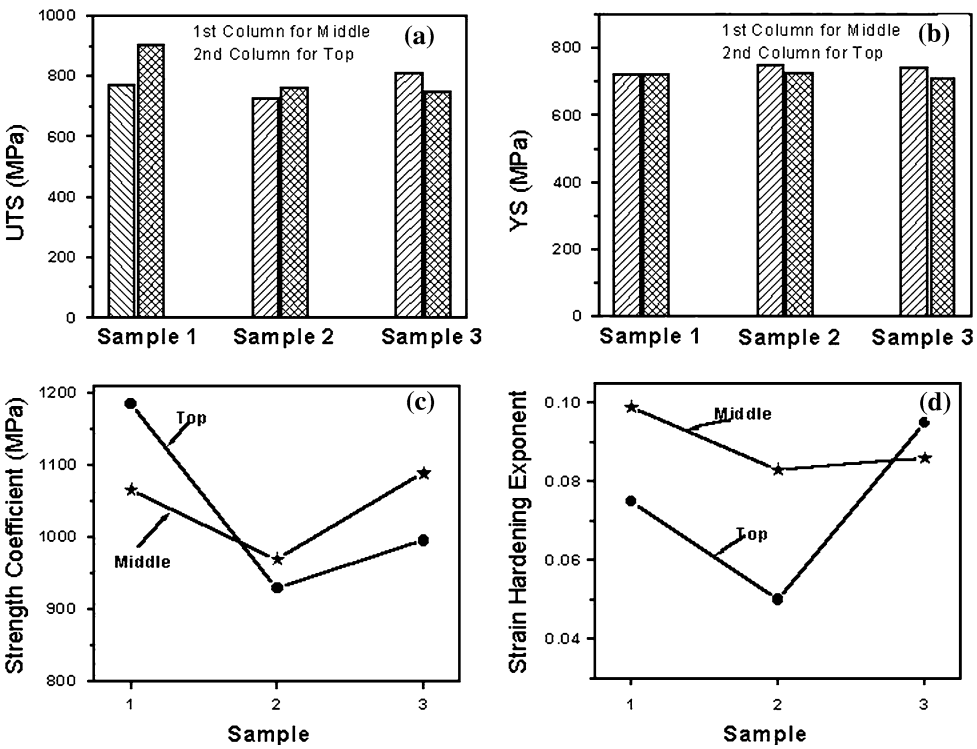

Fig. 10 Comparison of (**a**) UTS, (**b**) YS, (**c**) *K*, and (**d**) *n* values obtained from both top and middle position of the HAZs for samples '1', '2' and '3'

5. The variations in load–deflection curves of base, weld, and HAZ are consistent with their corresponding microstructure.

Acknowledgements The authors are grateful to Prof. S. P. Mehrotra, Director, National Metallurgical Laboratory (NML), for his encouragement and permission to carry out and publish this work. They are also thankful to Dr. I. Chattoraj and Dr. G. V. S. Murthy of NML for their valuable assistance. One of the authors (Sabita Ghosh) thanks the Council of Scientific & Industrial Research (CSIR), India, for a fellowship to carry out this work.

References

1. Webster PJ (1992) Welding handbook, 8th edn. American Welding Society, Miami
2. Hara T, Asahi H (2000) Corrosion 56:533
3. Bala Srinivasan P, Sharkawy SW, Dietzel W (2004) Mater Sci Eng A 385:6. doi:10.1016/j.msea.2004.03.029
4. Brass AM, Chêne J (2006) Corros Sci 48:481. doi:10.1016/j.corsci.2005.01.007
5. Carter TJ, Cornish LA (2001) Eng Fail Anal 8:113. doi:10.1016/S1350-6307(99)00040-0
6. Haggag FM, Byun TS, Hong JH, Miraglia PQ, Murty KL (1998) Scr Mater 38:645. doi:10.1016/S1359-6462(98)00519-3
7. Murty KL, Miraglia PQ, Mathew MD, Shah VN, Haggag FM (1999) Int J Pres Ves Pip 76:361. doi:10.1016/S0308-0161(99)00006-X
8. Haggag FM (2001) Residual stress measurement and general non-destructive evaluation. ASME 429:99
9. Byun TS, Hong JH, Haggag FM, Farrell K, Lee FH (1997) Int J Pres Ves Pip 74:231. doi:10.1016/S0308-0161(97)00114-2
10. Oliver WC, Pharr GM (1992) J Mater Res 7(5):1564
11. Bolshakov A, Pharr GM (1998) J Mater Res 13(4):1049
12. Oliver WC, Pharr GM (2004) J Mater Res 19(1):3
13. Field JS, Swain MV (1995) J Mater Res 10(1):101
14. Norbury AL, Samuel T (1928) JISI 117:673
15. Alcala J, Barone AC, Anglanda M (2000) Acta Mater 48:3451. doi:10.1016/S1359-6454(00)00140-3
16. Jang J-I, Choi Y, Lee Y-H, Kim D-J, Kim J-T (2003) J Mater Sci Lett 22:499. doi:10.1023/A:1022926100980
17. Das G, Ghosh S, Sahay SK, Ranganath VR, Vaze KK (2003) Trans Indian Inst Met 56(5):465
18. Das G, Ghosh S, Ghosh S (2006) NDT Int 39:155. doi:10.1016/j.ndteint.2005.06.011
19. Tabor D (1951) The hardness of metals. Clarendon Press, Oxford
20. Haggag FM, Namstad RK, Hutton JT, Thomas DL, Swain RL (1990) ASTM 1092, Philadelphia, p 188
21. Timoshenko S (1934) Theory of elasticity. McGraw Hill, New York
22. Dieter GE (1998) Mechanical metallurgy. McGraw-Hill Book Company, Singapore
23. Meyer E (1908) Z Ver Dtsch Ing 52:645
24. Mathew MD, Murty KL, Rao KBS, Mannan SL (1999) Mater Sci Eng A 264:159. doi:10.1016/S0921-5093(98)01098-3
25. Das G, Ghosh S, Sahay SK, Ranganath VR, Vaze KK (2004) Int J Mater Res Adv Tech Metallkunde 95:1120
26. Das G, Ghosh S, Ghosh S, Ghosh RN (2005) Mater Sci Eng A 408:158. doi:10.1016/j.msea.2005.07.026
27. Das G, Ghosh S, Sahay SK (2005) Mater Lett 59(18):2246. doi:10.1016/j.matlet.2005.01.074
28. Das G, Ghosh S, Bose SC, Ghosh S (2006) Mater Sci Eng A 424:326. doi:10.1016/j.msea.2006.03.011